ARMY RESEARCH LABORATORY

Effect of Annealing Temperature on the Ballistic Limit Velocity of Ti-6A1-4V ELI

by M. S. Burkins, W. W. Love,
and J. R. Wood

ARL-MR-359

August 1997

19971002 050

Army Research Laboratory

Aberdeen Proving Ground, MD 21005-5066

Effect of Annealing Temperature on the Ballistic Limit Velocity of Ti-6A1-4V ELI

M. S. Burkins
Weapons and Materials Research Directorate, ARL

W. W. Love, J. R. Wood
RMI Titanium Company

DTIC QUALITY INSPECTED 4

Abstract

Although titanium alloys have been used successfully in aircraft for many years, the relatively high cost of titanium coupled with the limited information on its ballistic properties has prevented widespread use in ground vehicles. In order to provide this ballistic information to vehicle designers, the U.S. Army Research Laboratory (ARL) and the RMI Titanium Company (RMI) performed a joint research program to evaluate the effect of annealing temperature on Ti-6Al-4V alloy, extra-low interstitial (ELI) grade, currently specified by MIL-A-46077D for armor use for the U.S. Army. RMI provided the plates, performed the annealing, and collected mechanical and microstructural information. ARL then tested the plates with the 20-mm fragment-simulating projectile (FSP) in order to determine the response of limit velocity as annealing temperature was varied from 732–1,038°C. This report summarizes information presented at ASM International Aeromat '96 Conference in Dayton, OH, in June 1996 and at the 16th International Symposium on Ballistics in San Francisco, CA, in September 1996.

Table of Contents

INTENTIONALLY LEFT BLANK.

List of Figures

INTENTIONALLY LEFT BLANK.

List of Tables

1. Introduction

Although titanium alloys have been used successfully in aircraft for many years, the relatively high cost of titanium coupled with the limited information on its ballistic properties has prevented widespread use of titanium in ground vehicles. As early as 1950, Pitler and Hurlich (1950) noted that titanium showed promise as a structural armor against small-arms projectiles. By 1964, the Ti-6Al-4V alloy, extra-low interstitial (ELI) grade had become the material of choice for armor applications. Ballistic testing had indicated that reductions in interstitial elements, such as carbon, oxygen, nitrogen, and hydrogen, improved the ductility and, hence, the ballistic protection of the plate (Sliney 1964). Consequently, the MIL-A-46077 armor specification was developed for ELI grade Ti-6Al-V; however, the effect of heat treatment on ballistic performance was never completely explored, and further research was hampered by a titanium production methodology that was still in its infancy.

In order to provide this basic information to vehicle designers, the U.S. Army Research Laboratory (ARL) and the RMI Titanium Company (RMI) performed a joint research program to evaluate the effect of annealing temperature on the ballistic limit velocity of Ti-6Al-4V ELI grade. RMI provided the plates, performed the annealing, and collected mechanical and microstructural information. ARL then tested the plates with the 20-mm fragment-simulating projectile (FSP) in order to determine the ballistic limit velocity of each plate. The ballistic limit velocity of the titanium plates was observed as a response to varying the annealing cycle.

2. Background

Titanium can exist in a hexagonal close-packed crystal structure (known as the alpha phase) and a body-centered cubic structure (known as the beta phase). In unalloyed titanium, the alpha phase is stable at all temperatures up to 882° C, whereupon it transforms to the beta phase. This transformation temperature is known as the beta transus temperature. The beta phase is stable from 882° C to the melting point (Donachie 1989).

1

As alloying elements are added to pure titanium, the phase transformation temperature and the proportions of each phase change. Alloy additions to titanium, except tin and zirconium, tend to stabilize either the alpha or beta phase. Ti-6Al-4V, the most common titanium alloy, contains mixtures of alpha and beta phases and is therefore classified as an alpha-beta alloy. The aluminum is an alpha stabilizer, which stabilizes the alpha phase to higher temperatures, and the vanadium is a beta stabilizer, which stabilizes the beta phase to lower temperatures. The addition of these alloying elements raises the beta transus temperature to approximately 996° C. Alpha-beta alloys, such as Ti-6Al-4V, are of interest for armor applications because they are generally weldable, can be heat treated, and offer moderate to high strengths (Donachie 1989).

Ti-6Al-4V can be ordered to a variety of commercial and military specifications. Plates manufactured to armor specification MIL-A-46077D were selected for this analysis because it is the only "off-the-shelf" armor alloy. This specification defines alloy chemistry ranges, minimum mechanical properties, and ballistic requirements. The chemical composition and minimum mechanical properties are listed in Tables 1 and 2, respectively. Transverse properties are determined from samples taken perpendicular to the final rolling direction.

Table 1. Chemical Composition for MIL-A-46077D Titanium Armor by Weight Percent

	Al	V	C	O	N	H	Fe	Other	Ti
Allowable Ranges	5.5–6.5	3.5–4.5	0.04 max.	0.14 max.	0.02 max.	0.0125 max.	0.25 max.	0.40 max.	Balance
As Delivered	6.12	4.02	0.01	0.12	0.008	0.0058	0.19	<0.40	Balance

NOTES: Al - aluminum, V - vanadium, C - carbon, O - oxygen, N - nitrogen, H - hydrogen, Fe - iron, Ti - titanium, and max. - maximum.

Table 2. Minimum Transverse Mechanical Properties for 28.5-mm-Thick MIL-A-46077D Titanium Armor

Ultimate Tensile Strength (MPa)	Yield Strength, 0.2% Offset (MPa)	Elongation (%)	Reduction in Area (%)
862	793	12	25

Starting from a single Ti-6Al-4V ELI grade plate, RMI produced a large 28.5-mm thickness plate by 1:1 cross rolling at temperatures below the beta transus. This plate then received a vacuum creep flatten (VCF) treatment to flatten and stress-relieve the plate. The cycle is approximately 24 hr, including heat-up and cool-down time, and reaches a temperature of 788° C. The plate was then cut into 11 305-mm × 457-mm test samples. Ten of these smaller plates received additional heat treatments, while one plate was left untreated to serve as the experimental control. RMI sandblasted and pickled all plates to remove the alpha case (oxide layer) and cut a corner from all 11 panels for tensile testing and metallographic examination.

3. Test Projectile

The 20-mm FSP (Figure 1) was selected as the test projectile for a number of reasons. Prior data by Sliney (1964) indicated that FSPs were better at showing differences in titanium performance than armor-piercing (AP) projectiles. Furthermore, the existing database was not as extensive for the 20-mm FSP as for AP projectiles. Finally, the FSP simulates the steel fragments ejected from high explosive artillery rounds, which remain a reasonable threat for many modern armors.
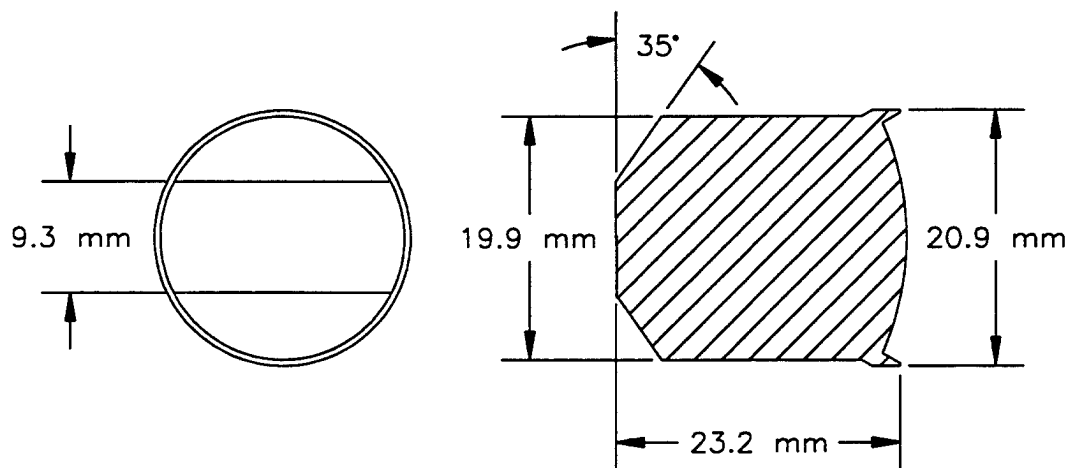
Figure 1. 20-mm FSP.

The 20-mm FSP was manufactured from 4340H steel, R_C 29–31 hardness, in accordance with specification MIL-P-46593A. A number of firings were conducted against each armor plate to determine a ballistic limit velocity. The 20-mm FSP was fired from a 20-mm rifled Mann barrel and the propellant load was varied in order to vary velocity. At least one projectile diameter of undisturbed material was maintained between adjacent projectile impacts on the plate.

4. Test Methodology

A schematic of the target setup is shown in Figure 2. Projectile velocities were measured using an orthogonal flash x-ray system developed by Grabarek and Herr (1966). The titanium plates were placed so that the projectile impacted normal to the plate (0° obliquity). The orthogonal pair of x-ray tubes permitted the measurement of projectile velocity, vertical pitch, and horizontal yaw just prior to impacting the titanium plate. A single pair of x-ray tubes was used to measure the velocity and length of any projectile or target fragments ejected from the rear surface of the target plate. The perforation of a paper break screen initiated the flash x-rays. Whenever possible, the residual penetrator and target material ejected from the rear were collected for analysis.
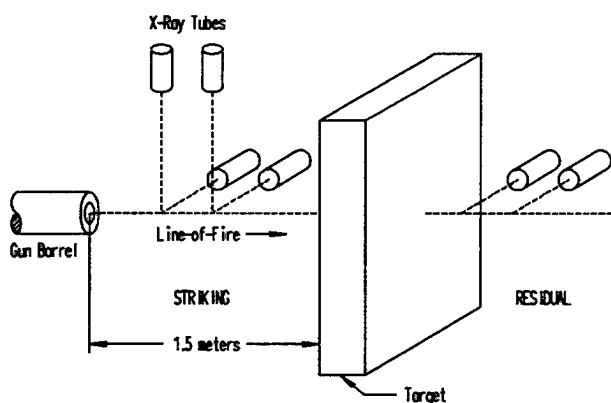
Figure 2. Schematic of Test Setup.

4

Testing was performed to obtain a V_{50} ballistic limit velocity, hereafter referred to as a V_{50}. The methodology for obtaining a V_{50} is explained in U.S. Army Test and Evaluation Command (TECOM) Test Operating Procedure (TOP) 2-2-710 (1993), but will be summarized here. The V_{50} is obtained by holding target thickness and obliquity constant, while varying projectile velocity by adjusting the weight of propellant. When a projectile impacts a target, the result is either a complete penetration (CP) or a partial penetration (PP). For this test, a CP occurred whenever a piece of penetrator or target material perforated the rear break screen, initiating the behind-armor x-rays and recording its image. A PP is any fair impact that is not a CP. Any PP result where the total yaw (vector sum of vertical pitch and horizontal yaw) was greater than 5° was considered an unfair impact and excluded from analysis in order to keep projectile orientation from influencing the results.

As projectile velocity is increased, a transition from PPs to CPs is generally observed. If a sufficient number of shots are fired, assuming that the target-penetrator interaction can be modeled by a cumulative normal (Gaussian) distribution, a mean (V_{50}) and standard deviation can be determined. The V_{50} was determined using equal numbers of PP and CP results over a designated velocity range specified by the MIL-A-46077 titanium armor specification.

In tests of eight of the plates, the V_{50} was determined from only six shots, consisting of the three highest PPs and three lowest CPs within a velocity spread of 27 m/s required by the armor test specification. For the tests of the other three plates, the initial velocity spread exceeded 27 m/s; therefore, testing was continued until a 10-shot V_{50} could be determined using the five highest PPs and five lowest CPs. The goal was for the velocity spread to be less than 39 m/s, but the water-quenched plate had a velocity spread of 59 m/s, and the VCF-only plate had a velocity spread of 42 m/s.

5. Metallographic Analysis

A sample was taken from each of the 11 plates in order to perform metallographic analysis and mechanical tensile testing. Photomicrographs and tensile testing data are provided in Appendix A.

5

Table 3 provides a summary of the microstructural data for the 11 plates tested. The first column provides the temperature and duration of the annealing cycle, as well as the cooling method. The different cooling rates were tested in order to provide some limited data on ballistic performance as a function of quenching rate. One plate was given a duplex anneal consisting of a beta anneal followed by an additional anneal below the beta transus. The second column lists the observed microstructures, which were typical of Ti-6Al-4V when annealed at the various conditions. The nine plates annealed at temperatures below the beta transus had a grain size of 10 per the American Society for Testing of Materials (ASTM) (ASTM E112-80). For the two plates annealed at temperatures above the beta transus, the grain size substantially increased to an ASTM grain size of <1 (approximately 0.25 mm).

Table 3. Microstructural Data for Ti-6Al-4V ELI Plates in Various Annealed Conditions

VCF Only, No Anneal 732° C, 30 min, AC 788° C, 30 min, AC 788° C, 30 min, WQ	Partially recrystallized alpha phase plus intergranular beta phase.
843° C, 30 min, AC 843° C, 2 hr, AC 899° C, 30 min, AC 954° C, 30 min, AC	Predominately equiaxed alpha phase with progressively increasing amounts of beta phase as annealing temperature increases.
899° C, 30 min, FC	In comparison to the AC plate annealed at the same temperature, the intergranular beta phase is reduced by the growth of alpha grains during slow cool.
1,038° C- 30 min, AC 1,038° C- 30 min, AC +788° C- 30 min, AC	Coarse prior beta grains that have transformed to a Widmanstätten alpha-beta microstructure.

NOTES: AC - air cooling, WQ - water quenching, and FC - 8-hr furnace cool.

Table 4 provides a listing of the average static tensile properties, as well as the Charpy V-Notch results, for the 11 plates tested. The minimum specification requirements are listed in the bottom line for comparison. Note that the specification has requirements for transverse properties only.

Table 4. Mechanical Properties for Ti-6Al-4V ELI Plates in Various Annealed Conditions

Anneal Cycle	Tensile Properties Longitudinal and Transverse								Charpy V-Notch	
	UTS (MPa)		YS (MPa)		Elong (%)		RA (%)		Energy (J)	
	L	T	L	T	L	T	L	T	TL	LT
VCF Only, No Anneal	972	904	897	831	15	15	38	28	27	29
732° C, 30 min, AC	951	911	884	833	14	13	43	29	26	27
788° C, 30 min, AC	986	917	938	863	15	13	37	30	27	27
788° C, 30 min, WQ	980	893	801	704	16	14	41	29	22	20
843° C, 30 min, AC	973	920	894	827	15	12	40	25	27	35
843° C, 2 hr, AC	984	926	901	836	14	14	37	32	33	38
899° C, 30 min, AC	999	962	911	944	13	11	32	28	37	31
899° C, 30 min, FC	960	899	896	834	16	14	41	31	33	33
954° C, 30 min, AC	962	920	861	807	14	15	42	37	45	42
1,038° C, 30 min, AC	950	951	816	817	10	10	18	17	46	45
1,038° C, 30 min, AC +788° C, 30 min, AC	940	930	838	826	9	9	17	18	39	39
MIL-A-46077 Min. Requirements	—	862	—	793	—	12	—	25	—	—

NOTES: UTS - ultimate tensile strength, YS - yield strength, Elong - elongation, RA - reduction in area, L - longitudinal, T - transverse, AC - air cooling, WQ - water quenching, FC - 8-hr furnace cool, and min - minimum. Double-lined boxes indicate properties below the requirement.

Average properties which were below the specification requirements are highlighted in the table. Only the failures to meet the reduction in area (RA) requirement appeared to have any correlation with poor ballistic results. Charpy results did not correlate with ballistic performance, as had been noted in some prior work (Sliney 1964).

6. Results

The 11 plates were tested with the 20-mm FSP, and V_{50} limit velocities were obtained for all plates. Table 5 lists the heat treatments, plate thicknesses, V_{50} limit velocities, and standard deviations. Detailed ballistic test data is included in Appendix B. Since the thickness of the plates varied slightly, the V_{50} results had to be normalized to a single reference thickness, in this case 28.58 mm (1.125 in). The mechanism chosen for normalizing the data was the limit velocity vs. thickness tables developed for the MIL-A-46077 specification. By utilizing the MIL-A-46077 table for the 20-mm FSP, along with some additional firing data, a linear approximation was developed for the relationship of limit velocity vs. plate thickness. Equation (1) provides an excellent approximation for the thickness range of 28.0 mm to 28.7 mm:

$$V_{50} = 37.85T - 1.366 \tag{1}$$

where T is the thickness in millimeters, and V_{50} is in meters per second.

Using equation (1), a normalization equation could be developed to correct the tested V_{50} limit velocities to a uniform 28.58-mm-thick plate. Equation (2) is the normalization equation:

$$V_{NORM} = V_{TEST} - 37.85T + 1,082, \tag{2}$$

where T is plate thickness in millimeters, V_{NORM} is the normalized V_{50} in meters per second, and V_{TEST} is the V_{50} obtained through testing in meters per second.

The greater the difference between the actual plate thickness and 28.58 mm, the larger the correction that was applied. A plot of the normalized V_{50} limit velocity vs. annealing temperature can be found in Figure 3.

Table 5. V_{50} **Ballistic Limit Test Results for Ti-6Al-4V ELI Plates in Various Annealed Conditions**

| Anneal Cycle	Thickness (mm)	Tested V_{50} (m/s)	Std Dev (m/s)	Normalized V_{50} (m/s)
VCF Only, No Anneal	28.55	1,111	13	1,112
732° C, 30 min, AC	28.22	1,085	8	1,099
788° C, 30 min, AC	28.27	1,106	7	1,118
788° C, 30 min, WQ	28.45	1,087	19	1,092
843° C, 30 min, AC	28.27	1,106	9	1,118
843° C, 2 hr, AC	28.47	1,120	10	1,124
899° C, 30 min, AC	28.30	1,130	8	1,141
899° C, 30 min, FC	28.17	1,117	8	1,133
954° C, 30 min, AC	28.47	1,098	10	1,102
1,038° C, 30 min, AC	28.45	810	7	815
1,038° C, 30 min, AC +788° C, 30 min, AC	28.07	795	9	815
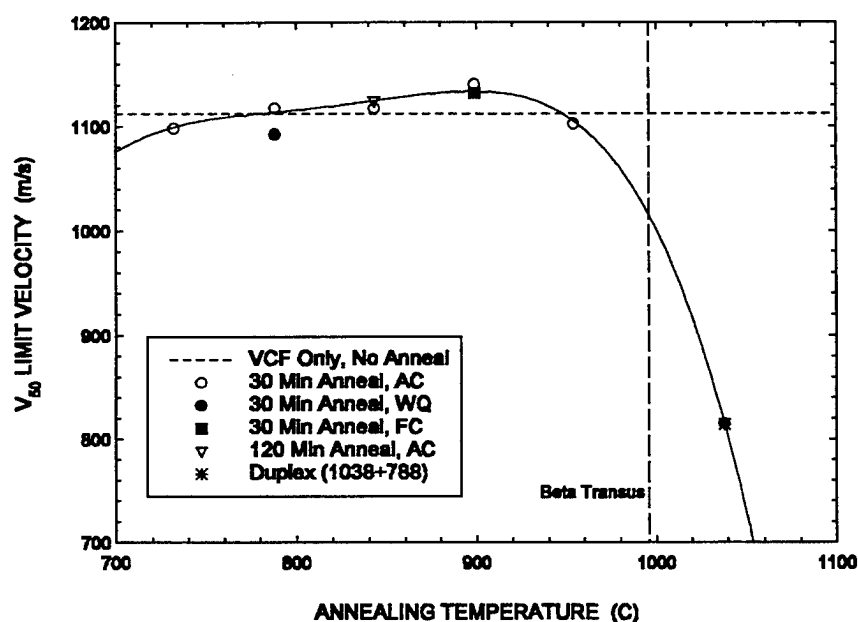
Figure 3. Normalized V_{50} Limit Velocity as a Function of Annealing Temperature.

9

As can be seen in Figure 3, plates annealed below the 996° C beta transus showed much higher V_{50} ballistic limit velocities than the plates annealed above the beta transus. The plate that received the VCF only without an additional anneal gave a performance comparable to most of the plates annealed below the beta transus. Although the conventional mill practice is to anneal in the 700–800° C temperature range, the highest limit velocity was obtained with an anneal at approximately 900° C. Thus, the data show that either the anneal step could be omitted to reduce cost or the anneal temperature could be increased to improve plate ballistic performance.

Since the limit velocities were significantly reduced for the plates annealed above the beta transus, an investigation of the failure modes of the plates seemed warranted. Figure 4a shows a 2× view of an impact crater in the VCF-only plate when the projectile striking velocity was 1,106 m/s, near the V_{50} limit velocity. Note the bulk deformation of the target material and the rear surface bulging. In addition, this plate showed a pattern of delaminations perpendicular to the projectile path and adiabatic shear failures parallel to the direction of fire. This was typical in all of the plates annealed below the beta transus. Figure 4b shows an increased magnification (50×) view of one of the adiabatic shear bands.

The failure mode for the plates annealed above the beta transus was quite different than for those annealed below the beta transus. Figure 5a shows a 2× view of the sectioned impact crater in the 1,038° C, 30 min, AC plate when the penetrator impact velocity was 813 m/s, near the limit velocity. Unlike the previous case, there is very little bulk deformation and bulging of the plate. The delamination failures are also completely absent. The adiabatic shear bands are more pronounced and are visible in Figure 5b, a 50× enlarged view of the shear bands. For this beta annealed plate, the shear bands propagate through the entire thickness of the plate, but for the VCF-only plate, the shear bands appeared to be interrupted by the delaminations.
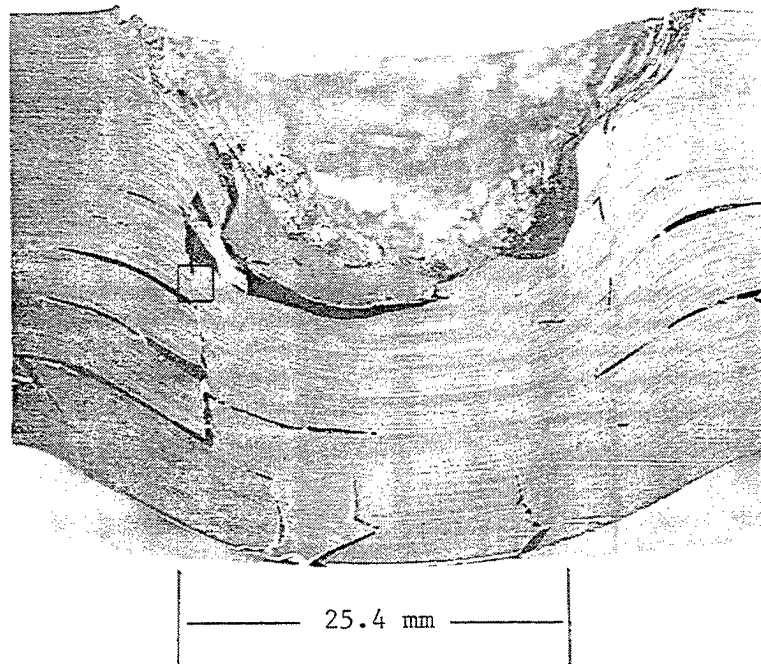
Figure 4a. Cross Section of Impact Crater in the VCF-Only Plate (2×).
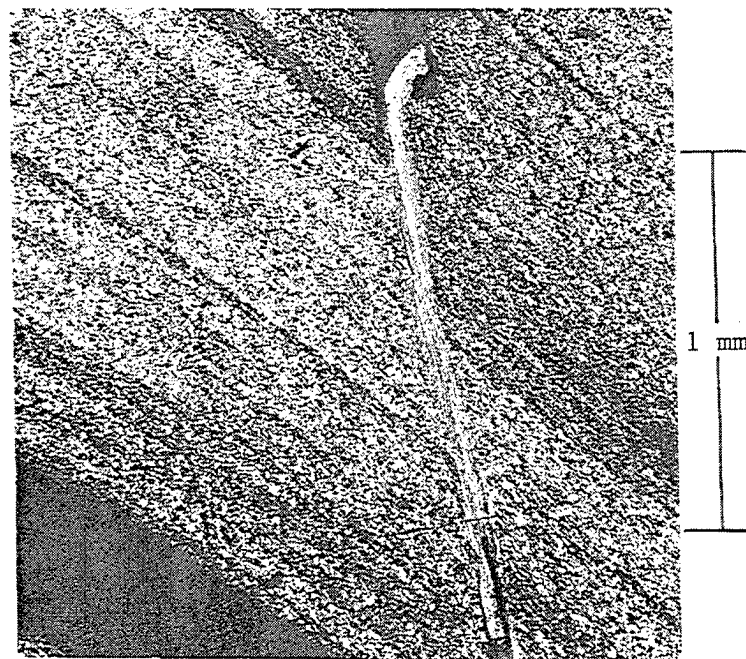

Figure 4b. Enlarged View Showing Adiabatic Shear Bands (50×).

11

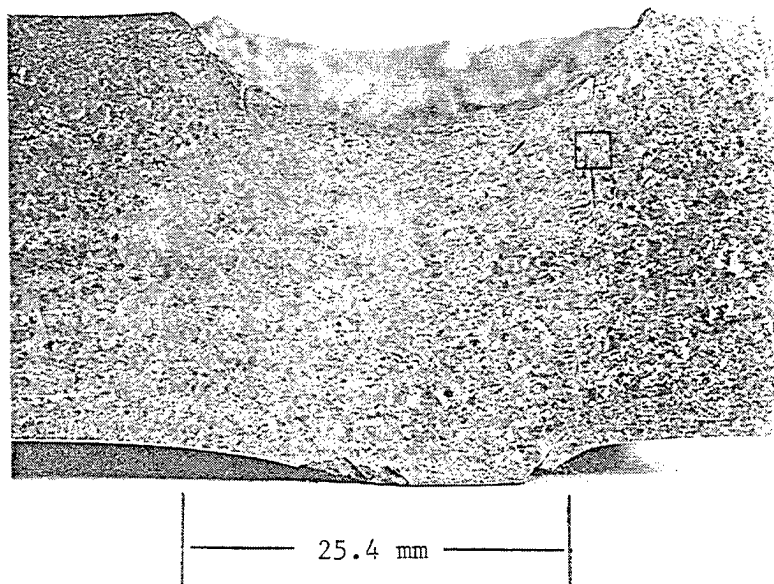**Figure 5a. Cross Section of Impact Crater in the 1,038° C, 30 min, AC Plate (2×).**
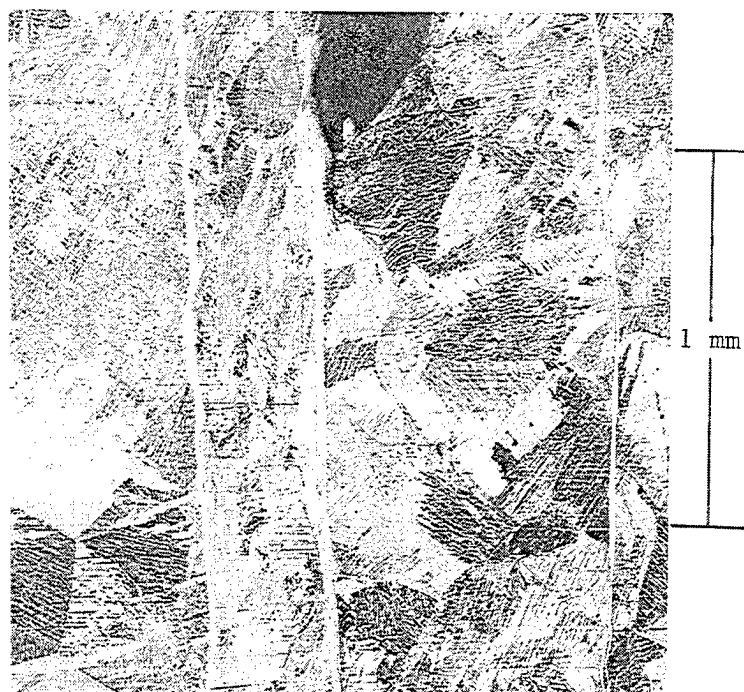
Figure 5b. Enlarged View Showing Adiabatic Shear Bands (50×).

12

This shear failure in beta annealed titanium had been noted by Corrigan (1961) and Koepke (1963). This low-energy failure mechanism permitted a cylindrical plug of titanium to be ejected from the titanium plate after approximately 3 mm of projectile penetration into the plate. The VCF-only plate, on the other hand, failed by spalling, the ejection of a thin disk of material after the projectile penetrated much deeper into the titanium plate.

7. Conclusions

Annealing Ti-6Al-4V ELI armor plate at temperatures above the beta transus significantly reduced the V_{50} ballistic limit velocity. This low-energy, shear-failure phenomenon was described by Corrigan (1961) and Koepke (1963). The V_{50} ballistic limit velocities were much higher and relatively insensitive to changes in annealing temperatures below the beta transus. The VCF-only plate, which received no additional anneal treatment, gave a performance comparable to most of the plates annealed below the beta transus. Although the conventional mill practice is to anneal in the 700–800° C temperature range, the highest limit velocity was obtained at approximately 900° C. Thus, the anneal step could be omitted to reduce cost, or the anneal temperature could be increased to improve plate ballistic performance. Additional work is contemplated to confirm that higher temperature annealing provides better ballistic performance in standard grade Ti-6Al-4V.

The failure modes of the beta and alpha-beta annealed plates were significantly different. The beta annealed plates failed by a process of adiabatic-shear plugging. This plugging was a low-energy failure mode that allowed a titanium plug to be ejected from the plate after the FSP had penetrated to a depth of approximately 3 mm into the armor. The plates annealed below the beta transus appeared to resist plugging failure, requiring the FSP to penetrate to a greater depth into the armor before the plate failed by a mixed process of bulging, delamination, shearing, and spalling.

INTENTIONALLY LEFT BLANK.

8. References

Corrigan, D. "Metallurgical Study of Titanium Alloy Armor, Part I- Ti-4Al-4V." WAL-TR-710.6/2 Pt. 1, Watertown Arsenal Laboratory, MA, January 1961.

Donachie, M. *Titanium: A Technical Guide.* ASM International, Metals Park, OH, 1989.

Grabarek, C., and E. L. Herr. "X-Ray Multi-Flash System for Measurement of Projectile Performance at the Target." BRL-TN-1634, U.S. Army Ballistic Research Laboratory, Aberdeen Proving Ground, MD, September 1966.

Koepke, B. "Metallurgical Study of Back Spall Formation in Ti-6Al-4V Armor Plate." WAL-TN-710.6/3, Watertown Arsenal Laboratory, MA, February 1963.

Pitler, R. and A. Hurlich. "Some Mechanical and Ballistic Properties of Titanium and Titanium Alloys." WAL-TR-401/17, Watertown Arsenal Laboratory, MA, March 1950.

Sliney, J. "Status and Potential of Titanium Armor." Proceedings of the Metallurgical Advisory Committee on Rolled Armor. AMRA S 64-04, USAMRA, January 1964.

U.S. Army Test and Evaluation Command. *Ballistic Tests of Armor Materials.* TOP-2-2-710 (AD A137873), Aberdeen Proving Ground, MD, 8 July 1993.

INTENTIONALLY LEFT BLANK.

Appendix A:

Metallographic Analysis and Tensile Testing Data

INTENTIONALLY LEFT BLANK.

Technical Memo 96-16

Evaluation of Ballistically Tested
Ti-6Al-4V ELI Armor Plate in
Various Annealed Conditions

J. R. Wood

EN 29002/ISO 9002/BS 5750
APPROVED BY BVQI

EN 29002/ISO 9002/BS 5750
APPROVED BY BVQI

EN 29002/ISO 9002
ANSI/ASQC Q92
APPROVED BY BVQI (NA)

Tech Memo 96-16

EVALUATION OF BALLISTICALLY TESTED Ti-6Al-4V ELI ARMOR PLATE IN VARIOUS ANNEALED CONDITIONS

INTRODUCTION

In 1993, an order was received from U.S. Army Research Lab, Aberdeen Proving Ground, Maryland, to provide Ti-6Al-4V ELI alpha-beta rolled plate sections - 1" x 12" x 18" with various annealing heat treatments for ballistic testing. A total of eleven (11) plates were shipped from Heat No. 854209 on M.O.s 13022-13032. The plates were ballistically tested by ARL in 1996 and small samples were returned to the RMI Technical Center for evaluation of microstructure and fracture characteristics.

PROCEDURE AND RESULTS

A description of the 11 annealed conditions of the as-shipped plates and the accompanying tensile, impact and double shear properties of each plate are shown in Table 1. Two plates (Travel Cards 67190 and 67189) were not given a separate anneal, but were supplied originally in the as-rolled plus vacuum creep flattened (VCF) condition ($\approx$1350°F-16hrs-furnace cool). One of these original plates was re-heat treated by ARL at 1650°F-30min-furnace cool and is designated as T.C. 67189A in Table 1. Samples of each plate were returned to RMI for metallographic examination and typical microstructures at 200X for each plate are shown in Figures 1 through 11.

The ballistic test results provided by ARL are shown in Table 2. The plates were shot with 20 mm fragment simulating projectile (FSP) rounds at different velocities and statistically analyzed for penetration. The V_{50} Limit Velocity shown in Table 2 is the projectile velocity associated with a 50% probability of complete penetration of the armor plate. The V_{50} value is commonly used to compare different armor materials. Four ballistically tested plate samples (T.C. 67190, 67193, 67186, 67184) were returned to RMI for evaluation of fracture characteristics. Photomicrographs at various magnifications are shown in Figures 12 through 15.

DISCUSSION

The microstructures in the various annealed conditions show a typical alpha-beta structure for Ti-6-4. At the lower annealing and VCF temperatures up to 1450°F, the structure consists of partially recrystallized alpha plase plus intergranular beta phase as shown in Figures 1 to 4. From 1550°F to 1750°F, the alpha phase becomes predominately equiaxed and progressively increasing amounts of beta phase appear as shown in Figures 5, 6, 7 and 9. Upon furnace cooling from 1650°F, as shown in Figure 8, the amount of intergranular beta phase is reduced (compared to Figure 7) by the growth of alpha grains during the slow cool. At 1900°F, which is approximately 75°F above the beta transus and is called a beta anneal, the structure consists of coarse prior beta grains which have transformed to a Widmanstätten alpha-beta microstructure,

RMI Titanium Company   2   Tech Memo 96-16

as shown in Figure 10. The additional 1450°F treatment used for T.C. 67183 serves as a stress relieve only and does not change the microstructure as shown in Figure 11.

Evaluation of the ballistically tested samples show similar failure modes for T.C.s 67190, 67193 and 67186 (Figures 12, 13 and 14, respectively). A series of parallel shear cracks are formed in the plane of the plate which link together in the direction of the projectile to cause significant deformation, bulging and cracking at the back surface. These separations appear to follow the elongated texture of the alpha-beta rolled and annealed structure. In Figures 12C, 13C and 14C there were thin layers of severely deformed metal between the major cracks. These are known as adiabatic shear bands which are layers of thermally softened material generated from the high deformation rates in ballistic testing[1,2].
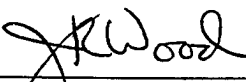
The deformation and fracture characteristics in T.C. 67184 which was beta annealed at 1900°F is slightly different from the previous samples as shown in Figure 15. Multiple shear cracks in layers were not evident, but instead a fewer number of vertical or 45° cracks were present. Adiabatic shear bands were visible adjacent to cracks as shown in Figure 15C.

CONCLUSIONS

This report is intended to describe the microstructural features of various annealed conditions in Ti-6-4 ELI plate. No attempt has been made to try to correlate mechanical properties or microstructure to ballistic test results, which is beyond the scope of this study.

APPROVAL

Written by: _____
J. R. Wood
Manager-Metals Research

Distribution
R&D Engineers
S. R. Giangiordano
W. W. Love
Matt Burkins - ARL

1.   H. Andrew Grebe, Han-Ryong Pak, and Marc A. Meyers, "Adiabatic Shear Localization in Titanium and Ti-6 Pct Al-4 Pct V Alloy", Met. Trans. A, Vol. 16A, May 1985, pp. 761-775.
2.   Raymond L. Woodward, "Metallographic Features Associated with the Penetration of Titanium Alloy Targets", Met. Trans. A, Vol. 10A, May 1979, pp. 569-573.

Table 1. Mechanical Properties of Plates in Various Annealed Conditions

T.C. No.	Anneal Cycle	Sample ID	Tensile Properties				CVN Impact Properties			Double Shear Strength ksi
			UTS ksi	YS ksi	EL %	RA %	Energy ft·lbs	MLE mils	Shear %	
67190	As VCF no H.T.	4L	140.9	130.1	15.0	37.9	20.0	10.0	20	87.3
		4T	131.1	120.5	15.0	28.0	21.0	7.0	25	
67189	As VCF no H.T.	5L	143.5	131.3	11.0	30.8	28.0	12.0	30	80.3
		5T	134.3	123.8	14.0	26.7	22.0	7.0	25	
67193	1350°F-30min-AC	1L	137.9	128.2	14.0	43.3	19.0	8.0	20	85.3
		1T	132.1	120.8	13.0	29.4	20.0	6.0	30	
67192	1450°F-30min-AC	2L	143.0	136.1	15.0	37.3	20.0	6.0	20	87.8
		2T	133.0	125.1	13.0	30.1	20.0	4.0	30	
67191	1450°F-30min-WQ	3L	142.2	116.1	16.0	41.0	16.0	5.0	30	79.9
		3T	129.5	102.1	14.0	29.4	15.0	4.0	20	
67188	1550°F-30min-AC	6L	141.1	129.7	15.0	39.9	20.0	7.0	25	87.8
		6T	133.4	120.0	12.0	25.3	26.0	9.0	30	
67187	1550°F-2hrs-AC	7L	142.7	130.7	14.0	37.1	24.0	9.0	20	86.6
		7T	134.3	121.2	14.0	32.8	28.0	12.0	30	
67186	1650°F-30min-AC	8L	144.9	132.1	13.0	31.6	27.0	13.0	40	77.8
		8T *	136.9	139.5	11.0	28.1	23.0	8.0	40	
67189A	1650°F-30min-fce cool*	5AL	139.2	129.9	15.9	40.5	24.0	NA	NA	NA
		5AT	130.4	121.0	13.7	30.5	24.5	NA	NA	
67185	1750°F-30min-AC	9L	139.5	124.9	14.0	41.5	33.0	15.0	50	85.0
		9T	133.4	117.0	15.0	37.1	31.0	12.0	30	
67184	1900°F-30min-AC	10L	137.8	118.3	10.0	17.6	34.0	14.0	30	83.7
		10T	137.9	118.5	10.0	16.8	33.0	16.0	30	
67183	1900°F-30min-AC + 1450°F-30min-AC	11L	136.3	121.5	9.0	16.8	29.0	12.0	30	82.1
		11T	134.9	119.8	9.0	18.3	29.0	12.0	25	

*Conducted by ARL.

* UTS & YS are transposed.

Table 2. Ballistic Test Results on RMI Annealed Plate

T.C. No.	Condition	V_{50} Limit Velocity (m/s)	Standard Deviation (m/s)	Sample Shipped to RMI
67190	VCF - No anneal	1114	13	Yes
67193	1350°F-30min-AC	1085	8	Yes
67192	1450°F-30min-AC	1106	7	No
67191	1450°F-30min-WQ	1087	19	No
67188	1550°F-30min-AC	1106	9	No
67187	1550°F-2hrs-AC	1120	10	No
67186	1650°F-30min-AC	1130	8	Yes
67189A	1650°F-30min-FC	1117	8	No
67185	1750°F-30min-AC	1100	12	No
67184	1900°F-30min-AC	810	6	Yes
67183	1900°F-30min-AC + 1450°F-30min-AC	795	9	No
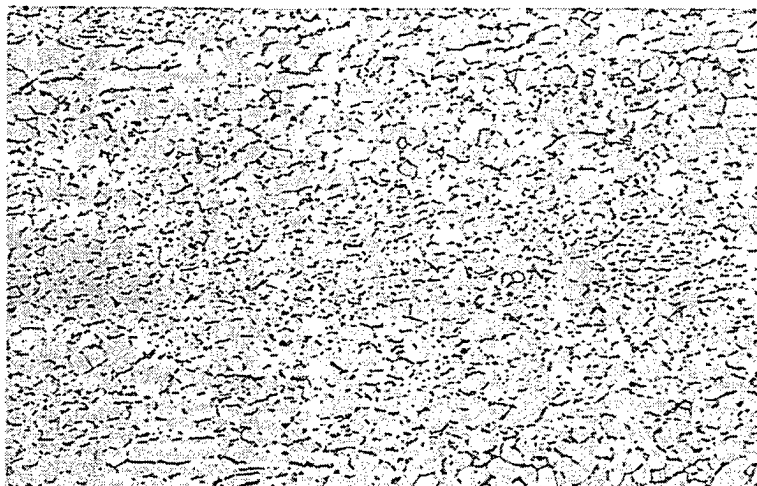
Figure 1.   T.C. 67190   VCF Only   200X

Figure 2.   T.C. 67193   1350°F-30min-AC   200X
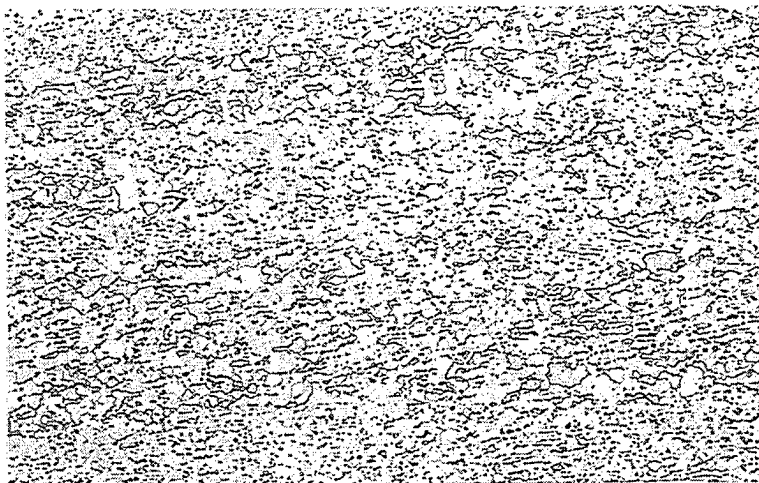
Figure 3.   T.C. 67192   1450°F-30min-AC   200X
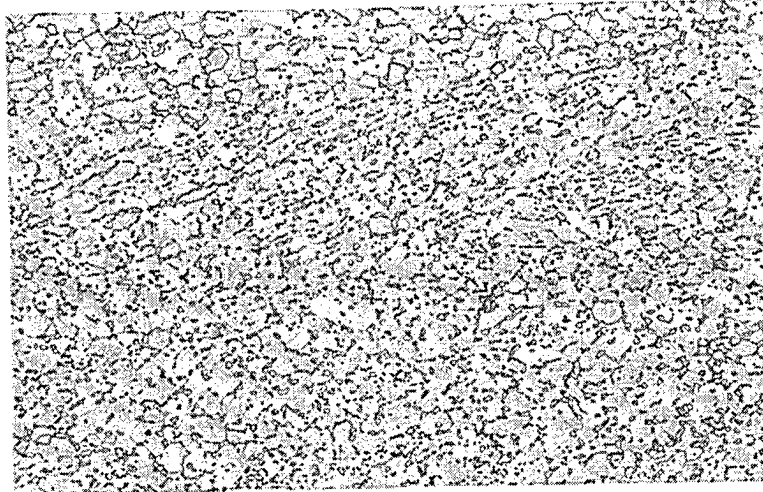
Figure 4.   T.C. 67191   1450°F-30min-WQ   200X

Figure 5.   T.C. 67188   1550°F-30min-AC   200X
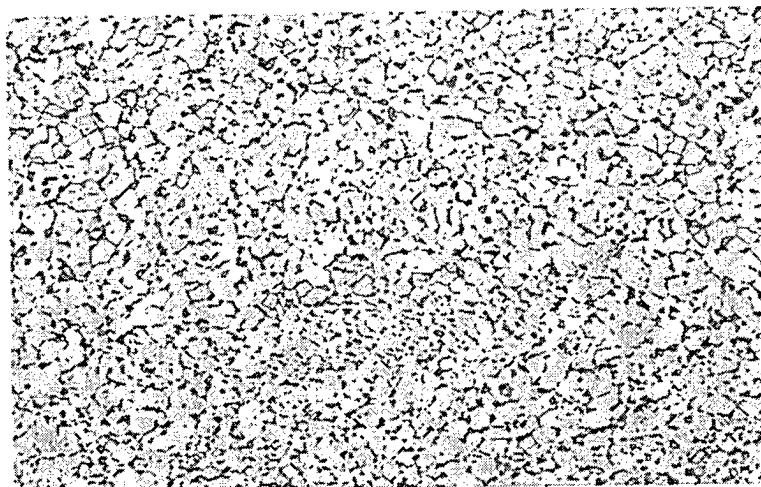
Figure 6.   T.C. 67187   1550°F-2hrs-AC   200X
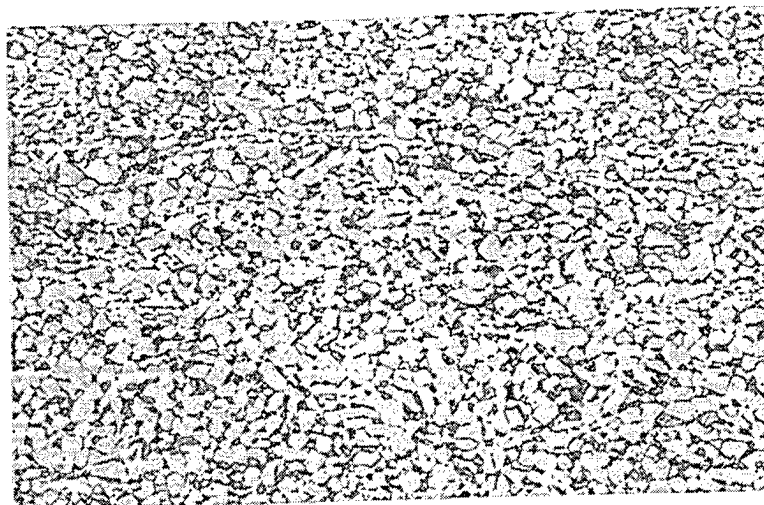
Figure 7.   T.C. 67186   1650°F-30min-AC   200X
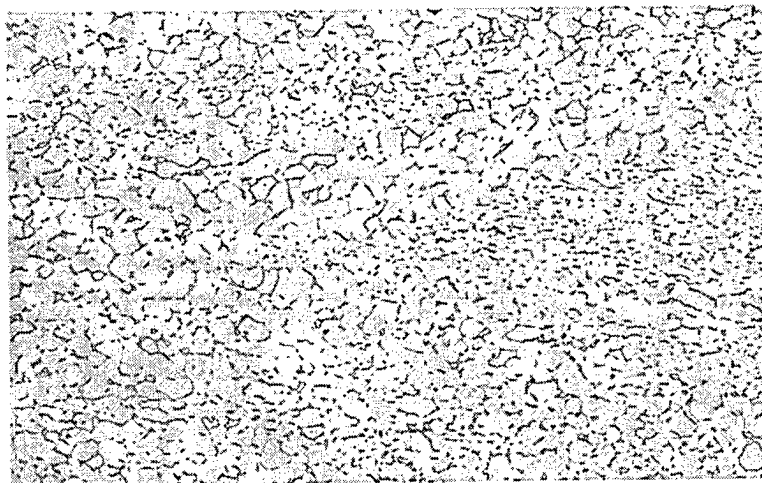
Figure 8. T.C. 67189A 1650°F-30min-Fce Cool 200X
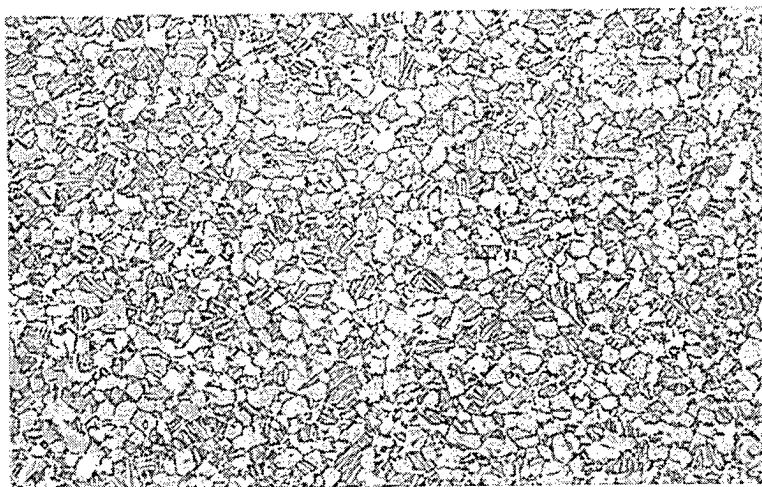
Figure 9.   T.C. 67185   1750°F-30min-AC   200X
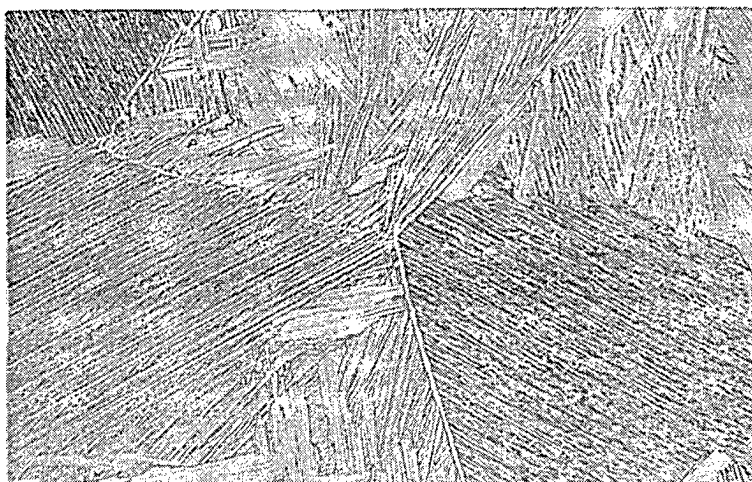
Figure 10.   T.C. 67184   1900°F-30min-AC   200X

Figure 11.   T.C. 67183   1900°F-30min-AC   200X
                              + 1450°F-30min-AC
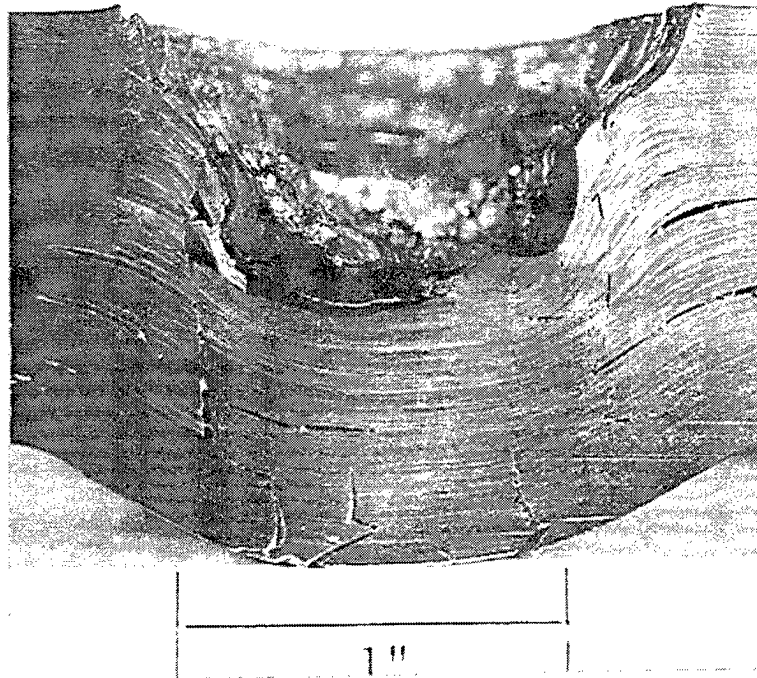
Figure 12A.   2X
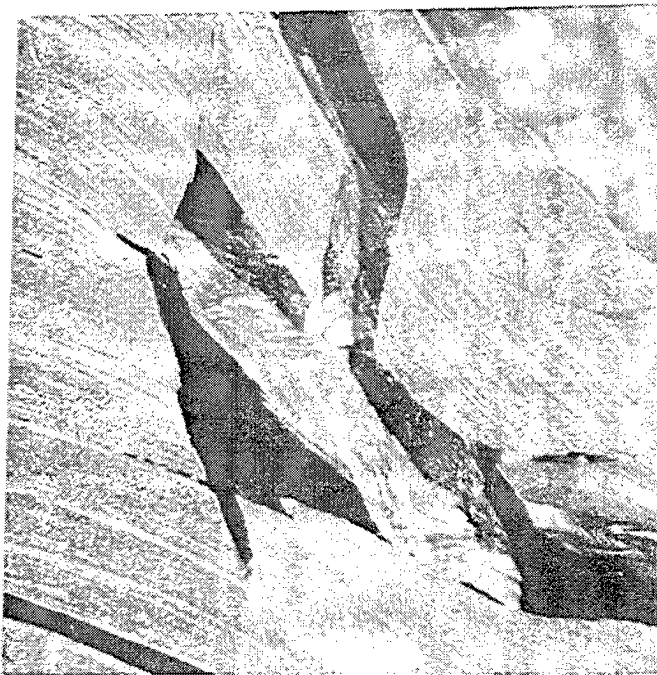
Figure 12B.   10X
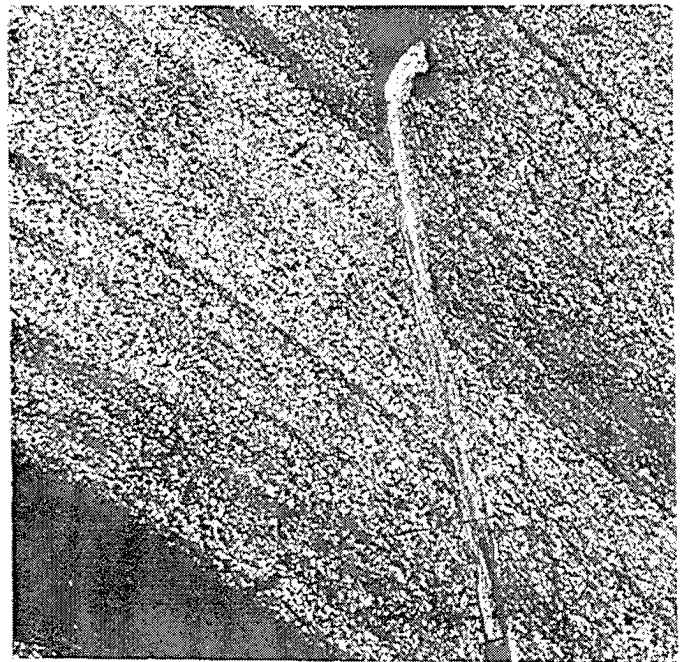
Figure 12C.   50X

Figure 12. Ballistic Fracture
T.C. 67190 VCF Only
$V_{50} = 1114$ m/s
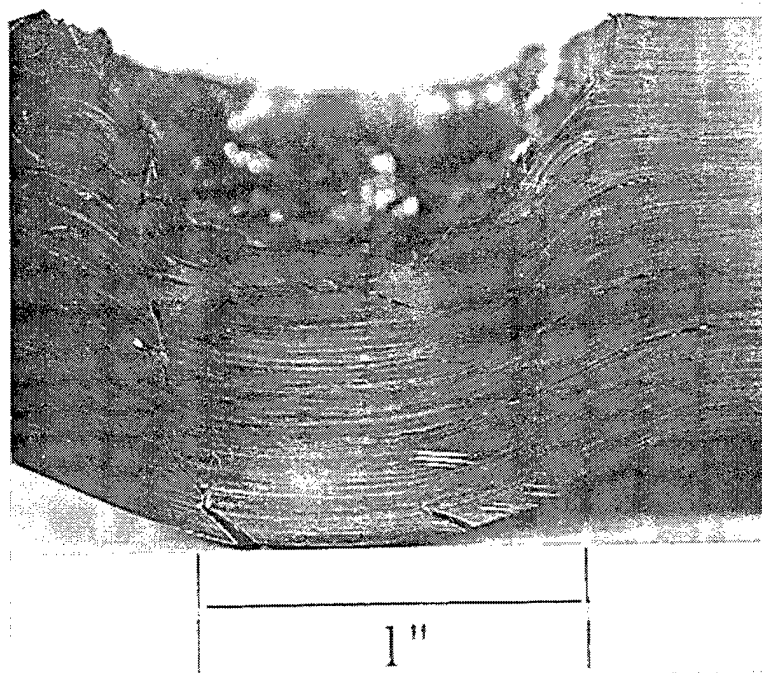
Figure 13A.   2X
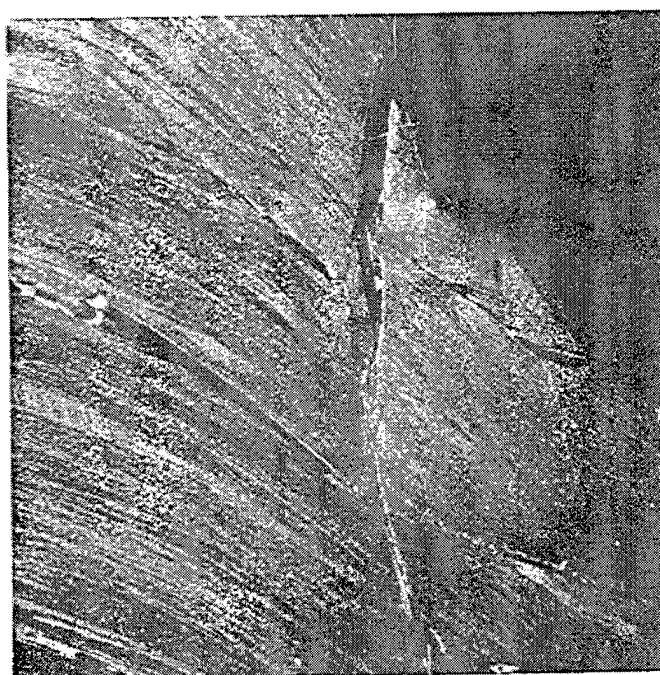
Figure 13B.   10X
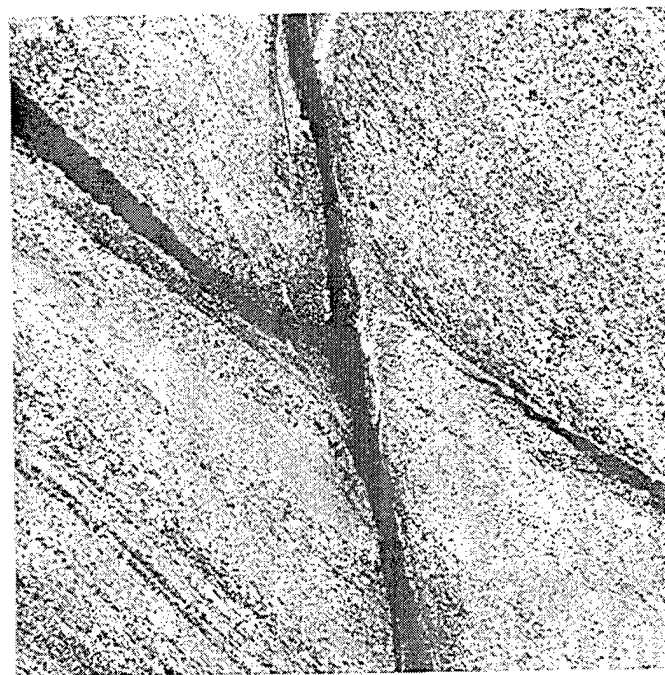
Figure 13C.   50X

Figure 13. Ballistic Fracture
T.C. 67193 1350°F-30min-AC
V_{50} = 1085 m/s
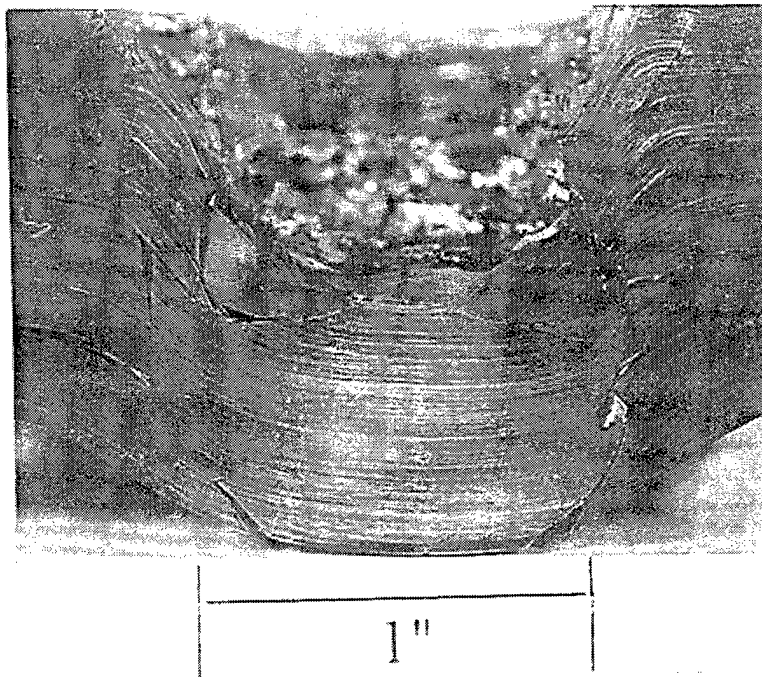
Figure 14A.   2X

Figure 14B.   10X
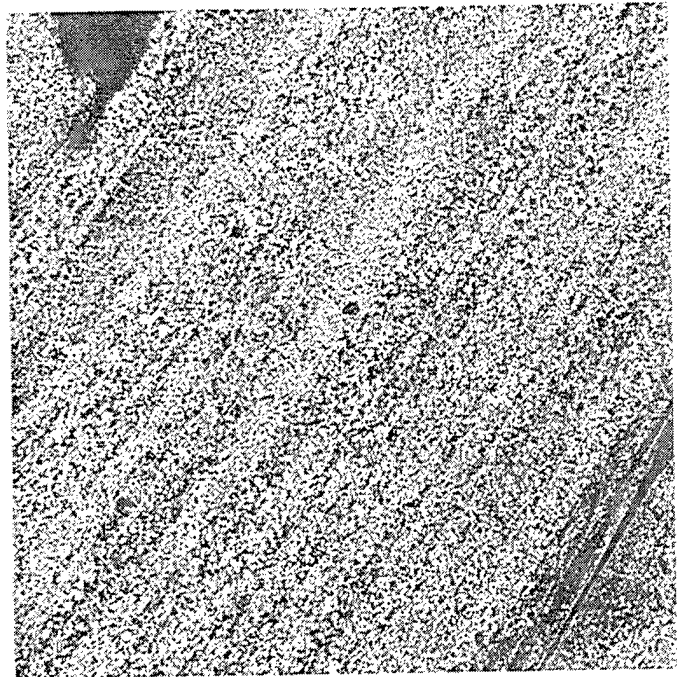
Figure 14C.   50X

Figure 14. Ballistic Fracture
T.C. 67186 1650°F-30min-AC
V_{50} = 1130 m/s
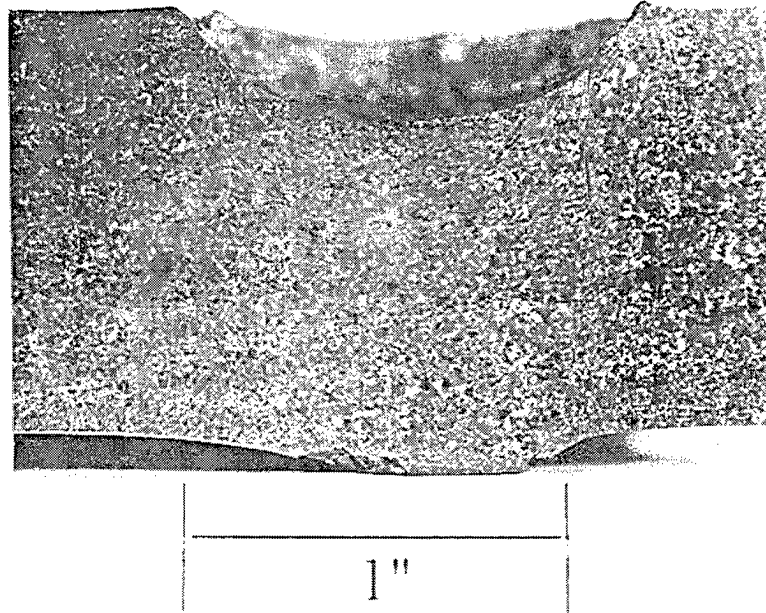
Figure 15A.   2X

Figure 15B.   10X   Figure 15C.   50X

Figure 15. Ballistic Fracture
T.C. 67184 1900°F-30min-AC
$V_{50} = 810$ m/s

INTENTIONALLY LEFT BLANK.

Appendix B:

Ballistic Test Data

INTENTIONALLY LEFT BLANK.

List of Abbreviations Used in this Appendix

—	Not applicable.
CP	Complete penetration; penetrator or target material exits the rear surface of the target. Asterisks (*CP*) indicate shots that were used to calculate the V_{50}.
ΔW	The mass loss in a plate caused by a shot. Mass of plate prior to shot minus the mass of plate after the shot.
L_R	Residual length; the length of residual penetrator or the thickness of a target material for a CP result.
M_R	Residual mass; the mass of residual penetrator or target material for a CP result.
NM	Not measured.
PIP	Penetrator in plate; penetrator lodged in impact crater.
PP	Partial penetration; the penetrator is defeated by the target. Asterisks (*PP*) indicate shots that were used to calculate the V_{50}.
P_R	Residual penetration; the impact crater depth.
RES	Result of shot; CP or PP.
V_R	Residual velocity; the velocity measured behind the target when a CP result occurs. The "COMMENTS" column defines whether this velocity is for penetrator or target material.
V_S	Striking velocity of projectile just prior to impacting the target.
YAW	Total yaw; the vector sum of vertical pitch and horizontal yaw for the projectile.

INTENTIONALLY LEFT BLANK.

Table B-1. Firing Data for 20-mm FSP vs. ELI Titanium Plate No. 67190 at 0° Obliquity (VCF Only, No Anneal; 28.55-mm thick; 286-BHN hardness)

Shot No.	V_S (m/s)	YAW (°)	RES	V_R (m/s)	L_R (mm)	M_R (g)	P_R (mm)	ΔW (g)	Comments
4011	823	1.41	PP	—	—	—	7	2.5	2-mm bulge
5645	890	1.06	PP	—	—	—	8	NM	2-mm bulge
4012	977	2.51	PP	—	—	—	11	24.3	5-mm bulge
4013	1,069	0.79	PP	—	—	—	15	18.0	8-mm bulge w/cracks
4015	1,089	0.79	PP	—	—	—	18	12.7	10-mm bulge w/cracks
5644	1,093	0.56	*PP*	—	—	—	17	NM	7-mm bulge w/cracks
4016	1,100	0.79	*PP*	—	—	—	21	21.8	11-mm bulge w/spall disk 50% formed
4024	1,102	0.71	*PP*	—	—	—	17.5	66.7	9-mm bulge w/cracks
4014	1,102	0	*CP*	25	6.3	22.9	—	65.0	Spall
4017	1,106	0.79	*PP*	—	—	—	17	23.2	9-mm bulge w/cracks
5643	1,106	1.03	*CP*	66	3	NM	18	NM	Spall
4019	1,118	0.35	*CP*	75	8.5	7.9	—	49.3	Spall
4010	1,119	0.56	*CP*	65	7.7	11.6	—	125	Spall
4020	1,131	0.25	*PP*	—	—	—	21	32.7	12-mm bulge w/spall disk 50% formed
4023	1,135	1.00	*CP*	102 127	14.0 29.5	38.8 38.7	—	114	Penetrator Spall
5642	1,135	0.50	CP	84	11.1	12.5	—	NM	Spall

Table B-2. Firing Data for 20-mm FSP vs. ELI Titanium Plate No. 67193 at 0° Obliquity (732° C, 30 min, AC; 28.22-mm thick; 293-BHN hardness)

Shot No.	V_S (m/s)	YAW (°)	RES	V_R (m/s)	L_R (mm)	M_R (g)	P_R (mm)	ΔW (g)	Comments
4021	1,003	1.12	PP	—	—	—	13.5	14.4	6-mm bulge w/cracks
4025	1,058	0.50	PP	—	—	—	16	20.2	8-mm bulge w/cracks
4027	1,075	0.56	*PP*	—	—	—	17	17.5	9-mm bulge w/cracks
4031	1,078	0	*PP*	—	—	—	17	21.8	9-mm bulge w/cracks
4026	1,081	1.00	*PP*	—	—	—	19	16.7	11-mm bulge w/spall disk 75% formed
4029	1,086	1.68	*CP*	12	9.5	34.8	—	53.8	Spall
4028	1,093	0.50	*CP*	50	7.2	23.1	—	120	Spall
4022	1,096	0.50	*CP*	92 / 97	14.0 / 18.5	37.5 / 45.8	—	116	Penetrator Spall
4030	1,123	0.35	CP	12 / 53	14.7 / 17.5	37.4 / 38.1	—	81.2	Penetrator Spall

Table B-3. Firing Data for 20-mm FSP vs. ELI Titanium Plate No. 67192 at 0° Obliquity (788° C, 30 min, AC; 28.27-mm thick; 286-BHN hardness)

Shot No.	V_S (m/s)	YAW (°)	RES	V_R (m/s)	L_R (mm)	M_R (g)	P_R (mm)	ΔW (g)	Comments
4285	1,053	0.79	PP	—	—	—	15.5	36.7	6-mm bulge w/crack
4286	1,093	1.03	PP	—	—	—	17	24.4	10-mm bulge w/cracks
4293	1,096	0.35	*PP*	—	—	—	19	19.0	11-mm bulge w/cracks
4288	1,098	0	*PP*	—	—	—	17	22.5	8-mm bulge w/cracks
4292	1,103	0.56	*PP*	—	—	—	19	20.6	11-mm bulge w/cracks
4291	1,107	0.56	*CP*	16	1	NM	22	20.8	Small chip ejected
4290	1,113	0.25	*CP*	185	1.6	0.04	19	25.5	Small chip ejected
4289	1,116	0.75	*CP*	132	2.5	0.16	20	28.2	Small chip ejected
4287	1,136	0	CP	67 / 89	13.6 / 17.7	40.0 / 56.7	—	90.8	Penetrator Spall
4284	1,151	0.35	CP	162 / 205	13.4 / 19.5	35.1 / 33.6	—	103	Penetrator Plug

Table B-4. Firing Data for 20-mm FSP vs. ELI Titanium Plate No. 67191 at 0° Obliquity (788° C, 30 min, WQ; 28.45-mm thick; 286-BHN hardness)

Shot No.	V_S (m/s)	YAW (°)	RES	V_R (m/s)	L_R (mm)	M_R (g)	P_R (mm)	ΔW (g)	Comments
4295	1,052	0.50	*CP*	184	1.9	0.08	14	28.3	Small chip ejected
4296	1,055	0.25	*PP*	—	—	—	15	17.3	8-mm bulge w/cracks
4297	1,079	0.79	*PP*	—	—	—	17	21.3	9-mm bulge w/cracks
4299	1,085	0	*PP*	—	—	—	17.5	17.6	9-mm bulge w/cracks
4302	1,087	0.56	*PP*	—	—	—	17	24.9	9-mm bulge w/cracks
4300	1,093	0	*PP*	—	—	—	18	29.0	10-mm bulge w/cracks
4301	1,100	0.25	*CP*	42	7.9	29.2	24	80.5	Spall
4310	1,100	1.46	*CP*	23 107	14.3 17.5	37.4 43.6	—	102	Penetrator Spall
4298	1,104	0.35	*CP*	72	18.4	59.0	—	128	Spall
4309	1,111	0.56	*CP*	75 90	14.0 19.8	39.1 41.0	—	104	Penetrator Spall
4294	1,150	0.35	CP	121 164	13.8 17.9	38.0 25.0	—	129	Penetrator Spall

Table B-5. Firing Data for 20-mm FSP vs. ELI Titanium Plate No. 67188 at 0° Obliquity (843° C, 30 min, AC; 28.27-mm thick; 286-BHN hardness)

Shot No.	V_S (m/s)	YAW (°)	RES	V_R (m/s)	L_R (mm)	M_R (g)	P_R (mm)	ΔW (g)	Comments
4263	913	2.02	PP	—	—	—	9	13.8	4-mm bulge
4264	963	2.02	PP	—	—	—	11.5	8.8	5-mm bulge
4265	1,071	0.90	PP	—	—	—	16	20.2	8-mm bulge w/cracks
4271	1,093	0.35	*PP*	—	—	—	17	23.1	4-mm bulge
4272	1,101	0.25	*PP*	—	—	—	17	18.8	5-mm bulge
4267	1,103	1.03	*PP*	—	—	—	18	19.9	9-mm bulge w/spall disk 40% formed
4270	1,106	0	*CP*	65	2	NM	23	25.1	Small chip ejected
4269	1,113	0.56	*CP*	53	18.1	58	—	120	Spall
4268	1,120	0.50	*CP*	161	2	NM	22	22.5	Small chip ejected
4266	1,139	0.56	CP	77	17.7	42.9	—	108	Spall
4262	1,168	1.25	CP	156 205	13.4 17.5	40.3 30.5	—	109	Penetrator Plug

Table B-6. Firing Data for 20-mm FSP vs. ELI Titanium Plate No. 67187 at 0° Obliquity (843° C, 2 hr, AC; 28.47-mm thick; 302-BHN hardness)

Shot No.	V_S (m/s)	YAW (°)	RES	V_R (m/s)	L_R (mm)	M_R (g)	P_R (mm)	ΔW (g)	Comments
4235	986	1.03	PP	—	—	—	12.5	18.0	5-mm bulge w/cracks
4236	1,101	0.56	*PP*	—	—	—	18	17.2	11-mm bulge w/spall disk 50% formed
4242	1,105	0.25	*PP*	—	—	—	18	18.3	9-mm bulge w/cracks
4247	1,116	0.56	*PP*	—	—	—	24	21.6	12-mm bulge w/spall disk 50% formed
4246	1,116	0.35	*CP*	80	2	NM	19	21.3	5-mm bulge w/cracks
4241	1,123	0.25	*CP*	47	18.4	40.5	—	115	11-mm bulge w/spall disk 50% formed
4238	1,125	0.75	*PP*	—	—	—	23	23.0	15-mm bulge w/plug pushed out 9 mm
4244	1,125	0.71	*CP*	33 55	13.6 18.8	35.4 57.4	—	84.1	Penetrator Plug
4239	1,128	0.25	*CP*	94	8.0	27.8	—	56.0	Spall
4245	1,129	0.50	*CP*	99 126	13.4 17.4	38.3 36.4	—	109	Penetrator Spall
4240	1,132	0.56	*PP*	—	—	—	22.5	27.8	11-mm bulge w/spall disk 25% formed
4237	1,143	0.35	CP	80	15.5	56.7	—	117	Spall
4243	1,168	2.15	CP	129 186	13.5 18.5	37.6 30.5	—	109	Penetrator Plug

Table B-7. Firing Data for 20-mm FSP vs. ELI Titanium Plate No. 67186 at 0° Obliquity (899° C, 30 min, AC; 28.30-mm thick; 293-BHN hardness)

Shot No.	V_S (m/s)	YAW (°)	RES	V_R (m/s)	L_R (mm)	M_R (g)	P_R (mm)	ΔW (g)	Comments
4274	996	0.71	PP	—	—	—	8	17.0	5-mm bulge
4275	1,048	1.58	PP	—	—	—	14	24.7	6-mm bulge w/crack
4276	1,100	0.79	PP	—	—	—	19.5	28.0	10-mm bulge w/spall disk 50% formed
4280	1,108	1.27	PP	—	—	—	22	20.7	13-mm bulge w/spall disk 75% formed
4278	1,119	1.52	*PP*	—	—	—	26	25.5	Spall disk 75% formed and pushed out 18-mm
4279	1,124	0.25	*PP*	—	—	—	20.5	26.1	12-mm bulge w/spall disk 40% formed
4281	1,127	0.56	*PP*	—	—	—	24	80.6	12-mm bulge w/spall disk 75% formed
4277	1,132	0.75	*CP*	61 70	13.7 17.9	38.7 60.2	—	92.8	Penetrator Plug
4282	1,133	1.03	*CP*	83 121	13.2 19.1	40.0 32.4	—	118	Penetrator Plug
4283	1,145	1.00	*CP*	92 125	13.2 19.2	35.4 45.0	—	88.5	Penetrator Plug
4273	1,162	0.56	CP	156 185	11.6 19.1	36.4 68.2	—	103	Penetrator Plug

Table B-8. Firing Data for 20-mm FSP vs. ELI Titanium Plate No. 67189A at 0° Obliquity (899° C, 30 min, FC; 28.17-mm thick; 293-BHN hardness)

Shot No.	V_S (m/s)	YAW (°)	RES	V_R (m/s)	L_R (mm)	M_R (g)	P_R (mm)	ΔW (g)	Comments
4674	1,107	1.77	*PP*	—	—	—	18	19.0	8-mm bulge w/cracks
4676	1,111	1.58	*PP*	—	—	—	24	48.0	16-mm bulge w/spall disk 60% formed
4678	1,111	0.25	*PP*	—	—	—	19	24.0	9-mm bulge w/cracks
4679	1,121	1.80	*CP*	104 129	13.4 17.1	39.5 35.3	—	114	Penetrator Plug
4677	1,125	0.90	*CP*	49	9.1	23.3	20.5	33.0	Spall
4675	1,127	0.35	*CP*	129 184	17.5 4.6	29.1 6.4		105	Plug Spall

Table B-9. Firing Data for 20-mm FSP vs. ELI Titanium Plate No. 67185 at 0° Obliquity (954° C, 30 min, AC; 28.47-mm thick; 302-BHN hardness)

Shot No.	V_S (m/s)	YAW (°)	RES	V_R (m/s)	L_R (mm)	M_R (g)	P_R (mm)	ΔW (g)	Comments
4043	799	1.80	PP	—	—	—	6.5	4.7	3-mm bulge
4044	1,062	1.46	PP	—	—	—	15	16.7	7-mm bulge w/cracks
4050	1,070	0.56	PP	—	—	—	18.5	17.0	11-mm bulge w/cracks
4047	1,086	0.25	*PP*	—	—	—	17	19.6	7-mm bulge w/cracks
4048	1,088	0.56	*PP*	—	—	—	32	39.0	Spall pushed out 13 mm
4046	1,095	0.56	*CP*	40	3	NM	17	21.5	Small chip ejected
4049	1,099	0.50	*PP*	—	—	—	17	33.9	10-mm bulge w/cracks
4045	1,109	0.50	*CP*	104	1	NM	—	28.0	Small chip ejected
5641	1,113	0.79	*CP*	137	8.0	15.4	—	NM	Spall
4052	1,120	1.50	CP	57 89 103	13.4 16.9 7.8	37.5 42.5 10.6	—	108	Penetrator Large spall Small spall
4051	1,121	0.50	CP	16	17.9	65.0	PIP	43.5	Spall

43

Table B-10. Firing Data for 20-mm FSP vs. ELI Titanium Plate No. 67184 at 0° Obliquity (1,038° C, 30 min, AC; 28.45-mm thick; 321-BHN hardness)

Shot No.	V_S (m/s)	YAW (°)	RES	V_R (m/s)	L_R (mm)	M_R (g)	P_R (mm)	ΔW (g)	Comments
4042	779	2.57	PP	—	—	—	7	7.4	4-mm bulge w/plug formed
4037	799	1.12	*PP*	—	—	—	8	4.2	4-mm bulge w/cracks
4038	806	1.41	*PP*	—	—	—	9	7.1	Plug pushed out 2 mm
4039	813	2.30	*PP*	—	—	—	8	11.4	4-mm bulge w/plug formed
4036	813	2.37	*CP*	85	2	NM	8	6.0	Small chip ejected
4041	814	1.12	*CP*	70	1	NM	8	1.8	Small chip ejected
4040	817	3.05	*CP*	103 130	4 6	NM NM	—	7.9	Small spall Large spall
4035	845	1.41	CP	208	3	NM	—	6.0	Spall
4034	866	2.36	CP	1	4.2	0.8	—	8.2	Small chip ejected
4033	994	1.58	CP	122 213	17 18.7	NM 32.0	—	85.3	Penetrator Plug
4032	1,100	0.90	CP	202 >241	14.1 19.6	39.6 24.8	—	120	Penetrator Plug

Table B-11. Firing Data for 20-mm FSP vs. ELI Titanium Plate No. 67183 at 0° Obliquity (1,038° C, 30 min, AC/788° C, 30 min, AC; 28.07-mm thick; 302-BHN hardness)

Shot No.	V_S (m/s)	YAW (°)	RES	V_R (m/s)	L_R (mm)	M_R (g)	P_R (mm)	ΔW (g)	Comments
4257	768	2.15	PP	———	—	—	6	5.8	3-mm bulge
4259	783	1.03	*CP*	LOST	2	NM	7	3.5	Small chip ejected
4256	784	1.46	PP	—	—	—	7	5.9	3-mm bulge w/cracks
4258	788	1.06	*PP*	—	—	—	7	4.3	4-mm bulge w/cracks
4260	796	1.12	*PP*	—	—	—	7	4.8	4-mm bulge w/plug formed
4255	796	1.12	*CP*	80	3	NM	7	9.2	Small chip ejected
4250	800	1.35	*PP*	—	—	—	6	6.4	4-mm bulge w/plug formed
4254	804	1.46	*CP*	125	2	NM	8	1.2	Small chip ejected
4253	808	2.06	CP	136	5	NM	7	6.4	Small chip ejected
4252	828	1.12	CP	138	3.2	0.5	8	6.5	Small chip ejected
4251	855	1.03	CP	85	24.7	54.6	—	64.1	Plug
4249	913	1.06	CP	42 143	23.7 8.8	33 0.6	—	57.5	Plug Spall
4248	1,142	0.71	CP	240 313	14.7 19.3	39.9 21.3	—	104	Penetrator Plug

45

INTENTIONALLY LEFT BLANK.

NO. OF COPIES	ORGANIZATION	NO. OF COPIES	ORGANIZATION
2	DEFENSE TECHNICAL INFORMATION CENTER DTIC DDA 8725 JOHN J KINGMAN RD STE 0944 FT BELVOIR VA 22060-6218	1	DPTY ASSIST SCY FOR R&T SARD TT T KILLION THE PENTAGON WASHINGTON DC 20310-0103
1	HQDA DAMO FDQ DENNIS SCHMIDT 400 ARMY PENTAGON WASHINGTON DC 20310-0460	1	OSD OUSD(A&T)/ODDDR&E(R) J LUPO THE PENTAGON WASHINGTON DC 20301-7100
1	CECOM SP & TRRSTRL COMMCTN DIV AMSEL RD ST MC M H SOICHER FT MONMOUTH NJ 07703-5203	1	INST FOR ADVNCD TCHNLGY THE UNIV OF TEXAS AT AUSTIN PO BOX 202797 AUSTIN TX 78720-2797
1	PRIN DPTY FOR TCHNLGY HQ US ARMY MATCOM AMCDCG T M FISETTE 5001 EISENHOWER AVE ALEXANDRIA VA 22333-0001	1	DUSD SPACE 1E765 J G MCNEFF 3900 DEFENSE PENTAGON WASHINGTON DC 20301-3900
1	PRIN DPTY FOR ACQUSTN HQS US ARMY MATCOM AMCDCG A D ADAMS 5001 EISENHOWER AVE ALEXANDRIA VA 22333-0001	1	USAASA MOAS AI W PARRON 9325 GUNSTON RD STE N319 FT BELVOIR VA 22060-5582
1	DPTY CG FOR RDE HQS US ARMY MATCOM AMCRD BG BEAUCHAMP 5001 EISENHOWER AVE ALEXANDRIA VA 22333-0001	1	CECOM PM GPS COL S YOUNG FT MONMOUTH NJ 07703
		1	GPS JOINT PROG OFC DIR COL J CLAY 2435 VELA WAY STE 1613 LOS ANGELES AFB CA 90245-5500
		1	ELECTRONIC SYS DIV DIR CECOM RDEC J NIEMELA FT MONMOUTH NJ 07703
1	ASST DPTY CG FOR RDE HQS US ARMY MATCOM AMCRD COL S MANESS 5001 EISENHOWER AVE ALEXANDRIA VA 22333-0001	3	DARPA L STOTTS J PENNELLA B KASPAR 3701 N FAIRFAX DR ARLINGTON VA 22203-1714